

1 Distorted wurtzite unit cells: Determination of lattice parameters of  
 2 non-polar *a*-plane AlGaN and estimation of solid phase Al content.

3 Masihhur R. Laskar<sup>a</sup>, Tapas Ganguli<sup>b</sup>, A. A. Rahman<sup>a</sup>, Amlan Mukherjee<sup>a</sup>, M. R. Gokhale<sup>a</sup>,  
 4 Arnab Bhattacharya<sup>a</sup>

5 <sup>a</sup>*Department of Condensed Matter Physics and Materials Science, Tata Institute of Fundamental Research,  
 6 Homi Bhabha Road, Mumbai 400005, India.*

7 <sup>b</sup>*Raja Ramanna Center for Advanced Technology, Indore 425013, India.*

## 8 Abstract

Unlike *c*-plane nitrides, “non-polar” nitrides grown in e.g. the *a*-plane or *m*-plane orientation encounter anisotropic in-plane strain due to the anisotropy in the lattice and thermal mismatch with the substrate or buffer layer. Such anisotropic strain results in a distortion of the wurtzite unit cell and creates difficulty in accurate determination of lattice parameters and solid phase group-III content ( $x_{solid}$ ) in ternary alloys. In this paper we show that the lattice distortion is orthorhombic, and outline a relatively simple procedure for measurement of lattice parameters of non-polar group III-nitrides epilayers from high resolution x-ray diffraction measurements. We derive an approximate expression for  $x_{solid}$  taking into account the anisotropic strain. We illustrate this using data for *a*-plane AlGaN, where we measure the lattice parameters and estimate the solid phase Al content, and also show that this method is applicable for *m*-plane structures as well.

9 *Keywords:* A1. High resolution X-ray diffraction; A3. Metalorganic vapor phase epitaxy; B1.  
 10 Non-polar; B2. Semiconducting III-V materials.

11 *PACS codes:* 81.05.Ea, 78.55.Cr, 81.15.Gh, 61.05.cp, 61.50.Ah

## 12 1. Introduction

13 Group III-nitrides semiconductors have potential applications in optoelectronics and mi-  
 14 croelectronics devices. Nitride semiconductors epilayers grown along the (0001) *c*-axis of the  
 15 wurtzite crystal structure suffer from strong undesirable spontaneous and piezoelectric polar-  
 16 ization fields, which give rise to internal electrical fields [1] and impair device performance. In  
 17 quantum wells these fields spatially separate the electrons and holes reducing the overlap of  
 18 their wave functions, and causing a reduction of the recombination efficiency and red-shift of  
 19 the emission peak in light-emitting devices [2]. A solution to avoid the deleterious polarization-  
 20 induced electric field effects is to use group-III nitride layers in crystal orientations which have  
 21 no polarization field in the growth direction, and hence across the device active region [3].  
 22 Therefore, there is extensive ongoing research towards the growth of “non-polar” (11̄20) *a*-plane  
 23 and (11̄00) *m*-plane ( $\perp c$ -axis) group III-nitrides. These non-polar *a*- or *m*-plane epilayers are  
 24 generally grown on *r*- or *m*-plane sapphire substrates respectively. The lattice mismatch and  
 25 thermal expansion coefficients of these nitride epilayers with respect to the substrate are differ-  
 26 ent along  $\parallel c$  and  $\perp c$ -directions. This gives rise to an *anisotropic* in-plane strain which distorts

27 the basal-plane of the hexagonal unit cell. Similar anisotropic differences in lattice mismatch  
28 and expansion coefficients also exist within the different members of the III-Nitride family, hence  
29 there is an anisotropic in-plane strain even when growing for example an *a*-plane AlGaN epi-  
30 layer on a *a*-plane GaN buffer layer. The distortion of the basal plane has also been observed  
31 for similar reason in case of *c*-plane GaN grown on *a*-plane sapphire substrate [4].

32 In *c*-plane oriented films, epilayers are under uniform in-plane strain, which deforms the unit  
33 cell but preserves the hexagonal symmetry of the basal plane. In that case the determination of  
34 lattice parameter and estimation of group III molar fraction in the ternary alloy (for example  
35 Al content of AlGaN films) is relatively straightforward [5, 6]. However, for the non-polar orien-  
36 tations, the anisotropic in-plane strain results a distortion of the wurtzite unit cell which breaks  
37 the hexagonal symmetry. Further, the orientation of the *a*-plane nitride epilayer on *r*-plane  
38 sapphire substrate results in a reduced number of available lattice points in the reciprocal space  
39 within the limiting-sphere that are accessible for diffraction measurements. This makes deter-  
40 mination of lattice parameters for non-polar nitrides and consequently the estimation of group  
41 III composition of non-polar nitrides very difficult [8, 9]. A few different procedures for lattice  
42 parameter determination of such structures have been discussed in the literature. Darakchieva  
43 et al. [8] detail a procedure that requires measuring several symmetric and skew-symmetric  
44 planes at multiple azimuth positions in an edge-symmetric geometry. Another approach by  
45 Roder et al.[9] uses measurements of interplanar spacings derived from a combination of 9 sym-  
46 metric, asymmetric, and skew-symmetric reflections, which are weighted by their corresponding  
47 fwhm values and used in a fitting routine to match to an orthorhombic structure via an error  
48 minimization routine. In this paper we suggest a slightly different procedure for measuring the  
49 lattice parameters for such distorted systems using high resolution x-ray diffraction (HRXRD).  
50 We first show that the anisotropic strain results in an orthorhombic distortion of the unit cell,  
51 and derive a general expression for the interplanar distance  $d_{hkl}$  in such structures. Using the  
52 interplanar distances determined from multiple symmetric and skew-symmetric reflections, we  
53 obtain the lattice parameters via a standard least-square error minimization routine that is eas-  
54 ily implemented in standard mathematical software packages using a matrix formulation. We  
55 also derive an approximate expression for the ternary alloy composition of  $\text{Al}_x\text{Ga}_{1-x}\text{N}$  epilayers,  
56 where the Al content  $x_{solid}$  is obtained solving the stress-strain tensor taking into account the  
57 anisotropic strain. The procedure is illustrated using measurements on *a*-plane AlGaN epilayers  
58 grown on AlN buffer layers on *r*-plane sapphire substrates. We also show that the procedure is  
59 applicable for *m*-plane nitrides as well.

## 60 2. Experiment

61 The AlGaN epilayers were grown via metal organic vapour phase epitaxy (MOVPE) in  
62 a  $3 \times 2''$  closed-coupled showerhead reactor. Trimethylgallium (TMGa), trimethylaluminium  
63 (TMAI), and ammonia ( $\text{NH}_3$ ) are used as precursors and Pd-diffused hydrogen ( $\text{H}_2$ ) as carrier  
64 gas. About  $0.8\mu\text{m}$  thick AlGaN epilayers were grown on AlN buffer layer. The details of  
65 the growth procedure can be found in Ref. [10]. The lattice parameters measurement were  
66 carried out by using a Philips X'PERT<sup>TM</sup> high resolution X-ray diffractometer with a symmetric  
67 Ge(220) hybrid monochromator and an asymmetric triple-axis analyzer and PIXcel solid state  
68 detector array. The  $2\theta$  value of a set of planes  $(11\bar{2}0)$ ,  $(2\bar{1}\bar{1}0)$ ,  $(\bar{1}2\bar{1}0)$ ,  $(10\bar{1}0)$ ,  $(21\bar{3}0)$ ,  $(2\bar{1}\bar{1}0)$ ,  
69  $(11\bar{2}0)$ ,  $(10\bar{1}1)$ ,  $(10\bar{1}2)$ ,  $(21\bar{3}1)$ ,  $(21\bar{3}2)$  were measured to confirm the orthorhombic distortion and

70 to estimate the lattice parameters. Absorption measurements were done on backside polished  
 71 samples using a Cary 5000 spectrophotometer to estimate the band gap of the epilayers.

### 72 3. Measurement of lattice parameters

73 Fig 1(a) shows a schematic diagram of the relative unit cell orientation of an *a*-plane III-  
 74 nitride epilayer on *r*-plane sapphire. The in-plane epitaxial relationships between the group  
 75 III-nitride layer and sapphire are  $[0001]_{nitride} \parallel [\bar{1}101]_{sapphire}$  and  $[1\bar{1}00]_{nitride} \parallel [11\bar{2}0]_{sapphire}$ .  
 76 The thermal expansion co-efficients in the respective directions and the lattice mismatch are  
 77 shown in the table 1. It is evident that the lattice and thermal mismatch along  $[0001]$  and  
 78  $[1\bar{1}00]$  are different which gives rise to the anisotropic strain in the overlayer and thus distorts  
 79 the basal plane of the unit cell as shown schematically in Fig 1(b-c) (solid line). Further, the  
 80 thermal mismatch along *c* ( $|\Delta\alpha_{[0001]}|$ ) and along *m* ( $|\Delta\alpha_{[1\bar{1}00]}|$ ) are larger for GaN/AlN compared  
 81 to the GaN/sapphire and AlN/sapphire cases.

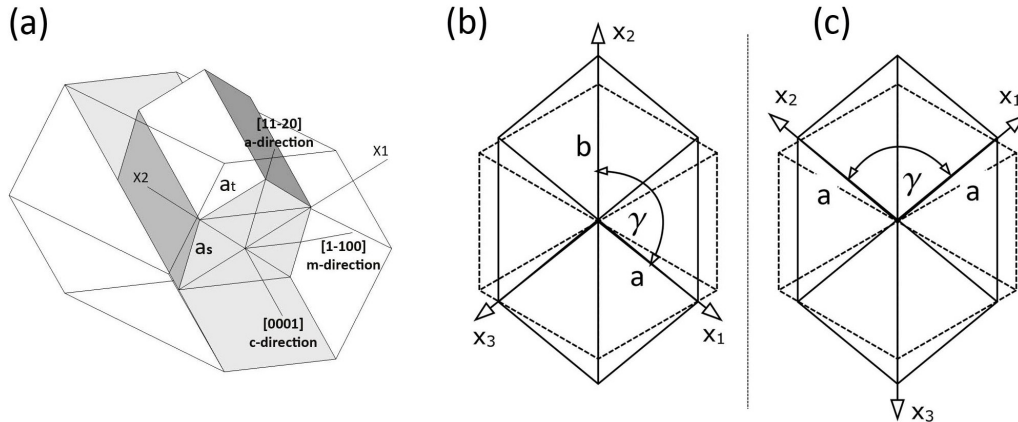


Figure 1: (a) Schematic diagram showing the orientation of wurtzite unit cell of  $(11\bar{2}0)$  *a*-plane oriented nitride epilayer on  $(\bar{1}\bar{1}01)$  *r*-plane sapphire substrate. Anisotropic in-plane strain results orthorhombic distortion and requires at least three lattice parameters  $a_s$  (sidewall),  $a_t$  (top) and  $c$  for complete description of the unit cell. (b-c) The dotted lines and solid lines show the basal plane of a perfect and distorted hexagonal unit cell respectively. (b) A choice of coordinate axis that involves four independent lattice variables  $a$ ,  $b$ ,  $c$  and  $\gamma$ , whereas in (c) symmetry allows the reduction of one parameter ( $a=b$ ) and gives a simpler expression for  $d_{hkl}$  and also helps to visualize the lattice points in the reciprocal space.

#### 82 3.1. Choice of coordinate axis

83 For a perfect hexagonal unit cell the inter-planar distance  $d_{hkl}$  (or  $d_{hki}$  where  $i = -h - k$ )  
 84 between the  $(hkl)$ -planes is given by  $1/d_{hkl}^2 = 4/3.[(h^2 + k^2 + hk)/a^2] + l^2/c^2$ . This expression  
 85 cannot be used for the distorted structure shown in Fig.1(b or c) (solid line). To obtain a  
 86 relatively simpler expression for new  $d_{hkl}$ , a proper choice of coordinate axis is helpful. In  
 87 the first choice [Fig 1(b)], the inter-planar lattice distance involves four independent lattice  
 88 variables  $a$ ,  $b$ ,  $c$ , and  $\gamma$ , so the expression of the  $d_{hkl}$  will be complicated. But for the second  
 89 choice [Fig. 1(c)], the symmetry in the distorted basal plane allows one to use  $a=b$  and reduce  
 90 one parameter thus simplifying the expression for the  $d_{hkl}$ . Further, such choice of coordinate  
 91 axis helps to visualize the lattice points in the reciprocal space, as discussed later in section 3.3.

Table 1: Thermal expansion and lattice mismatch

<i>Thermal expansion coefficient</i>	<i>GaN</i> ( $10^6 K^{-1}$ )	<i>AlN</i> ( $10^6 K^{-1}$ )	<i>Sapphire</i> ( $10^6 K^{-1}$ )	
$\alpha_{[0001]}$	3.17	5.27	-	
$\alpha_{[1\bar{1}00]}$	5.59	4.15	-	
$\alpha_{[\bar{1}101]}$	-	-	4.7	
$\alpha_{[11\bar{2}0]}$	-	-	4.5	
<i>Lattice mismatch</i>	% w.r.t. <i>GaN</i>	% w.r.t. <i>AlN</i>	% w.r.t. <i>Sapphire</i>	
	along <i>c</i>	along <i>m</i>	along <i>c</i>	along <i>m</i>
<i>GaN</i>	0	0	4.09	2.45
<i>AlN</i>	-3.92	-2.39	0	-2.87
			1.01	16.06
			-2.87	13.29

92 For the most general unit cell i.e. a triclinic structure, (Lattice sides  $a \neq b \neq c$  and angles  
93  $\alpha \neq \beta \neq \gamma$ ) the inter-planar lattice distance can be described by [12]

$$\frac{1}{d_{hkl}^2} = \frac{1}{V^2}(S_{11}h^2 + S_{22}k^2 + S_{33}l^2 + 2S_{12}hk + S_{23}kl + S_{13}hl)$$

$$V = abc\sqrt{1 - \cos^2 \alpha - \cos^2 \beta - \cos^2 \gamma - 2 \cos \alpha \cos \beta \cos \gamma}$$

$$S_{11} = b^2 c^2 \sin^2 \alpha$$

$$S_{22} = a^2 c^2 \sin^2 \beta$$

$$S_{33} = a^2 b^2 \sin^2 \gamma$$

$$S_{12} = abc^2(\cos \alpha \cos \beta - \cos \gamma)$$

$$S_{23} = a^2 bc(\cos \beta \cos \gamma - \cos \alpha)$$

$$S_{13} = ab^2 c(\cos \beta \cos \gamma - \cos \alpha)$$

94 For a hexagonal lattice with orthorhombic distortion, we can put  $\alpha = \beta = 90^\circ$  and  $a = b$ ,  
95 and thus obtain a simplified form

$$\frac{1}{d_{hkl}^2} = \frac{h^2 + k^2 - 2hk \cos \gamma}{(a \sin \gamma)^2} + \frac{l^2}{c^2} \quad (1)$$

96 The above expression for  $d_{hkl}$  is similar to that for an undistorted hexagonal structure, with  
97 additional terms  $\cos(\gamma)$  and  $\sin(\gamma)$  which take into accounts the distortion of the basal plane.

### 98 3.2. Accuracy in $d_{hkl}$ estimation

99 Throughout the experiment, the  $2\theta$  value for each plane was measured in the triple axis  
100 geometry and the interplanar distance  $d_{hkl}$  was estimated from the Bragg condition given by  
101  $d_{hkl} = \lambda/2 \sin \theta_{hkl}$ . If  $\Delta\theta$  is the error in the determination of peak position then the corre-  
102 sponding error in estimation of  $d$  is given by  $\Delta d = -d \cot \theta \Delta\theta$ . The error  $\Delta\theta$  can be minimized  
103 by careful optimization of the Eulerian cradle as discussed in [13]. To check the consistency in  
104 our measurements we repeated the measurement of the  $2\theta$  value for the  $(11\bar{2}0)$  reflection several

105 times by taking out the sample and reloading it. It was found that the change in  $2\theta$ -value occurs  
 106 in the third decimal place, which would lead to a corresponding change in the  $d$  value,  $\Delta d/d$ ,  
 107 of order  $10^{-5}$ . All our measurement are based on the accuracy of  $d_{hkl}$ -values up to the 4th  
 108 decimal place. Further, we have not incorporated a refractive index correction, and changes in  
 109  $d_{hkl}$ -values due to temperature fluctuations during the measurement (within  $5^\circ \text{C}$ ) which both  
 110 result in changes of  $\Delta d/d$ , of order  $10^{-5}$ .

### 111 3.3. Confirmation of orthorhombic distortion

112 We outline below a quick way to confirm the nature of distortion of the unit cell to be  
 113 orthorhombic. We choose the symmetric  $(11\bar{2}0)$  plane and its equivalent planes  $(2\bar{1}\bar{1}0)$  and  
 114  $(\bar{1}2\bar{1}0)$  which are easily accessible in skew-symmetric geometry by adjusting the rotational axis  
 115  $\phi$  and  $\psi$  ( $\phi$  is the angle of rotation about the normal to the sample mounting surface and  $\psi$   
 116 is the tilt of the diffracting plane out of the diffractometer plane). From the symmetry of the  
 117 wurtzite basal plane we expect that  $d_{11\bar{2}0}=d_{2\bar{1}\bar{1}0}=d_{\bar{1}2\bar{1}0}$  for an undistorted hexagon as shown in  
 118 Fig. 2a. Our measurements on a-plane GaN show that  $d_{11\bar{2}0} \geq d_{2\bar{1}\bar{1}0}=d_{\bar{1}2\bar{1}0}$  as schematically  
 119 shown in Fig. 2b(Data Shown in Table. 2). This implies that the unit cell gets compressed  
 120 along  $m$ -direction and elongated along  $a$ -direction. Hence the angle between the axis vector  $\mathbf{x}_1$   
 121 and  $\mathbf{x}_2$  is less than  $120^\circ$ . For  $a$ -plane epilayers the direct measurement of  $d_{1\bar{1}00}$  and  $d_{\bar{1}100}$  is not  
 122 possible because of geometry limitations of our diffractometer.

123 Further, the two skew-symmetric planes  $(10\bar{1}0)$ ,  $(01\bar{1}0)$  give identical  $2\theta$ -values (i.e.  $d_{10\bar{1}0} =$   
 124  $d_{01\bar{1}0}$ ). Since  $d_{10\bar{1}0}$  is the interplanar distance between BC and AO planes (Fig. 2), and  $d_{01\bar{1}0}$  is  
 125 the same between AB and OC -planes, so we can write OA=OC or  $a = b$ . We next choose a set  
 126 of asymmetric planes which involve the  $c$  lattice parameter, like  $(11\bar{2}2)$ ,  $(11\bar{2}\bar{2})$ ;  $(10\bar{1}1)$ ,  
 127  $(01\bar{1}1)$ ,  $(01\bar{1}\bar{1})$ ;  $(2\bar{1}\bar{1}2)$ ,  $(\bar{1}2\bar{1}2)$ ; we found that each set of asymmetric planes gives identical  
 128  $2\theta$ -value (within measurements error:  $\Delta\theta \pm 0.001^\circ$ ). Further, it is also found that the peak  
 129 positions of the  $(10\bar{1}0)$  and  $(01\bar{1}0)$  have the azimuthal relationship  $\phi_{10\bar{1}0} = \pm 180^\circ + \phi_{01\bar{1}0}$ ,  
 130 similar relationship holds true for  $(2\bar{1}\bar{1}0)$ ,  $(\bar{1}2\bar{1}0)$  planes also. These measurements confirm  
 131 that  $\alpha = \beta = 90^\circ$ . From these observations, we conclude that the hexagonal unit cell has  
 132 orthorhombic distortion.

Table 2: Confirmation of orthorhombic distortion.

Planes (hkil)	Measured value (distorted) $2\theta_{hkl}$ (degree)	Undistorted	
		$d_{hkl}$ (\AA)	$(d'_{hkl})$ (\AA)
$(11\bar{2}0)$	57.6378	1.5979	1.5947
$(2\bar{1}10)$	57.9779	1.5894	1.5947
$(\bar{1}2\bar{1}0)$	57.9769	1.5894	1.5947

### 133 3.4. Least square method

134 For an orthorhombic distorted hexagonal unit cell, we have derived an expression for the  
 135 inter-planar distance  $d_{hkl}$  (Eq.1). Since this expression has only three independent variables  $a$ ,  
 136  $c$ , and  $\gamma$ , these can be evaluated in principle by measuring the  $2\theta$ -values of only three reflections of  
 137 non-equivalent planes [for example  $(11\bar{2}0)$ ,  $(10\bar{1}0)$  and  $(10\bar{1}1)$ ] from which the lattice parameters

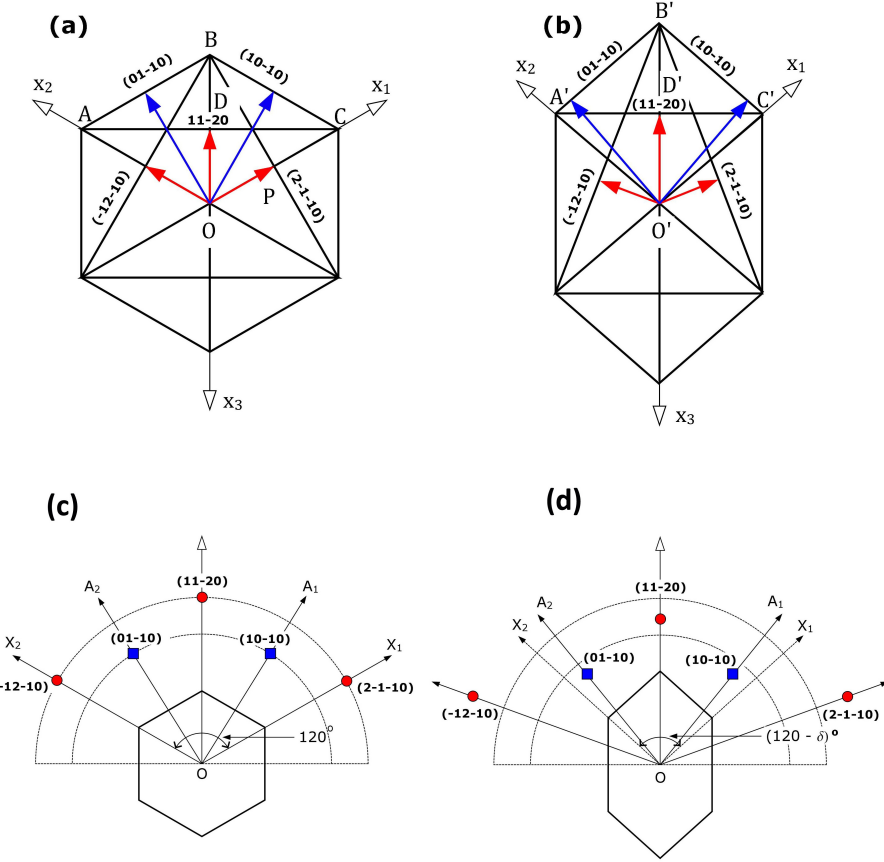


Figure 2: The diagram showing the basal plane of (a) perfect hexagonal and (b) orthorhombic distorted wurtzite unit cell. Different interplanar distance have been marked by arrows for both the structures, showing the inequalities. Reciprocal lattice points of (c) perfect hexagonal and (d) orthorhombic distorted structures.

138 can be estimated. But to improve the accuracy of measurement it is better to measure multiple  
139 reflections and minimize the error using a least square method.

140 Here we can write  $\gamma = 120^\circ - \delta$ . If  $|\delta|$  is small ( $\leq 1^\circ$ ), we can write  $\sin(\gamma) = \sin(120^\circ - \delta) =$   
141  $1/2(1 - \sqrt{3}\delta)$  and  $\cos(\gamma) = \cos(120^\circ - \delta) = \sqrt{3}/2(1 - \delta/\sqrt{3})$ . Substituting back to the eq(1),  
142 we can write an approximate expression:

$$\begin{aligned}
\frac{1}{d_{hkl}^2} &= \frac{h^2 + k^2 + hk(1 + \sqrt{3}\delta)}{\frac{3}{4}a^2 \left(1 - \frac{\delta}{\sqrt{3}}\right)^2} + \frac{l^2}{c^2} \\
&= \frac{4(h^2 + k^2 + hk(1 + \sqrt{3}\delta))}{3a^2} \left(1 - \frac{\delta}{\sqrt{3}}\right)^{-2} + \frac{l^2}{c^2} \\
&= \frac{4(h^2 + k^2 + hk(1 + \sqrt{3}\delta))}{3a^2} \left(1 + \frac{2\delta}{\sqrt{3}}\right) + \frac{l^2}{c^2} \\
&= \frac{4(h^2 + k^2 + hk)}{3a^2} + \frac{4}{3\sqrt{3}} \frac{(2h^2 + 2k^2 + 5hk)}{a^2} \delta + \frac{l^2}{c^2}
\end{aligned}$$

143 Here we have neglected the higher order  $\delta^2$ -term. By rearranging it, we can write the

<sup>144</sup> expression in the form of 3 linear variables:

$$\frac{1}{d_{hkl}^2} = \left[ \frac{4}{3}(h^2 + k^2 + hk) \right] \cdot \frac{1}{a^2} + \left[ \frac{4}{3\sqrt{3}}(2h^2 + 2k^2 + 5hk) \right] \cdot \frac{\delta}{a^2} + [l^2] \cdot \frac{1}{c^2} \quad (2)$$

<sup>145</sup> Assuming  $x_1 = 1/a^2$ ,  $x_2 = \delta/a^2$  and  $x_3 = 1/c^2$  we can express Eqn.(2) in a linear form  
<sup>146</sup> with variables  $x_1$ ,  $x_2$  and  $x_3$ . Now for a set of  $n$  reflecting planes say,  $(h_1, k_1, l_1)$ ,  $(h_2, k_2, l_2)$   
<sup>147</sup> .... $(h_n, k_n, l_n)$ ; we will get  $n$ -equations which can be expressed in a matrix form  $\mathbf{Ap}=\mathbf{D}$ , where  
<sup>148</sup>  $\mathbf{A}$  is a  $(3 \times n)$  matrix whose element  $[A]_{qj}$  is the co-efficients of the variable  $x_j$  ( $j = 1, 2, 3$ ) of the  
<sup>149</sup>  $q$ -th equation ( $q = 1, 2, \dots, n$ ),  $\mathbf{p}=(x_1 \ x_2 \ x_3)$ , and  $\mathbf{D}=(1/d_1^2 \ 1/d_2^2 \ \dots \ 1/d_n^2)^T$ , where  $d_n = d_{h_n k_n l_n}$   
<sup>150</sup> and T denotes transpose of the matrix. The required matrix,  $\mathbf{p}$ , whose elements contain the  
<sup>151</sup> lattice parameters can be obtained by solving the matrix equation  $\mathbf{p}=(\mathbf{A}^T \mathbf{A})^{-1} (\mathbf{A}^T \mathbf{D})$ . This  
<sup>152</sup> is of a form that can be easily implemented in standard software packages like Mathematica and  
<sup>153</sup> Matlab.

### <sup>154</sup> 3.5. Example

<sup>155</sup> For our  $a$ -plane GaN on AlN buffer layer, we have measured the  $2\theta$ -value of a set of nine  
<sup>156</sup> reflections as shown in Table 3 and then calculated the matrix  $\mathbf{A}$  and  $\mathbf{D}$ .

Table 3:  $2\theta$ -value for the set of planes for  $a$ -plane GaN

Planes	$2\theta_{hkl}$ (degree)	$d_{hkl}$ (Å)
(11̄20)	57.64	1.5980
(10̄10)	32.38	2.7628
(21̄30)	94.86	1.0459
(2̄110)	57.98	1.5894
(11̄22)	69.00	1.3600
(10̄11)	36.85	2.4373
(10̄12)	48.13	1.8889
(21̄31)	97.41	1.0253
(21̄32)	105.18	0.9698

<sup>157</sup>  $\mathbf{A} = \begin{pmatrix} 4.00 & -6.93 & 0.00 \\ 1.33 & -1.54 & 0.00 \\ 9.33 & -15.39 & 0.00 \\ 4.00 & -0.00 & 0.00 \\ 4.00 & -6.93 & 4.00 \\ 1.33 & -1.54 & 1.00 \\ 1.33 & -1.54 & 4.00 \\ 9.33 & -15.39 & 1.00 \\ 9.33 & -15.39 & 4.00 \end{pmatrix}; \text{ and } \mathbf{D} = \begin{pmatrix} 0.39 \\ 0.13 \\ 0.91 \\ 0.39 \\ 0.54 \\ 0.17 \\ 0.28 \\ 0.95 \\ 1.06 \end{pmatrix}.$

158 By solving the matrix equation for  $\mathbf{p}$  using Matlab, we obtain the solution for the lattice  
 159 parameters as  $a = 3.1788 \text{ \AA}$ ,  $c = 5.1774 \text{ \AA}$ , and with  $\delta = 0.36^\circ$ , with standard deviations for  
 160  $\sigma(a) = 2.9 \times 10^{-9}$ ,  $\sigma(c) = 6.2 \times 10^{-9}$  and  $\sigma(\delta) = 4.1 \times 10^{-8}$  respectively. We note that the value  
 161 of  $\delta$  obtained is small and satisfies the assumption of  $\delta \leq 1^\circ$ . Following the same procedure we  
 162 have estimated the lattice parameters for the set of  $a$ -plane AlGaN samples, details are shown  
 163 in Table 4.

164 *3.6. Procedure for  $m$ -plane structure*

165 In case of  $m$ -plane nitrides are grown on the  $m$ -plane sapphire substrates. Since the lattice  
 166 and thermal mismatch along  $c$  and  $a$ -axis are different, the distortion in the basal plane will be  
 167 similar to the  $a$ -plane nitrides. Figure 3(a) shows the orientation of unit cell of  $m$ -plane nitride  
 168 on  $m$ -plane sapphire substrate.

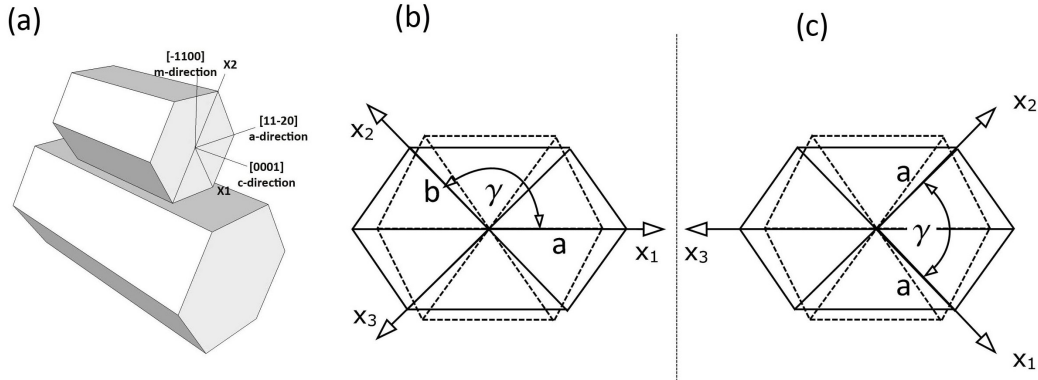


Figure 3: (a) Schematic diagram showing the orientation of wurtzite unit cell of  $(\bar{1}100)$   $m$ -plane oriented nitride epilayer on  $(\bar{1}100)$   $m$ -plane sapphire substrate. Anisotropic in-plane strain results in orthorhombic distortion. The dotted lines and solid line shows the basal plane of a perfect and distorted hexagonal unit cell respectively. (b) A choice of coordinate axis that involves four independent lattice variables  $a$ ,  $b$ ,  $c$  and  $\gamma$ , whereas in (c) symmetry allows the reduction of one parameter ( $a=b$ ) and gives a simpler expression for  $d_{hkl}$ .

169 As in the case of  $a$ -plane nitrides, an appropriate choice of coordinate axes can result in  
 170 a simpler form of  $d_{hkl}$ . The first choice (Fig.3b), the inter-planar lattice distance involves four  
 171 independent lattice variables  $a$ ,  $b$ ,  $c$ , and  $\gamma$ , whereas in the second choice (Fig. 3c), the symmetry  
 172 in the distorted basal plane allows one to use  $a=b$  and reduces one parameter resulting in a  
 173 simpler expression for  $d_{hkl}$  which is exactly identical to Eq(1). Also the distortion in the unit  
 174 cell can be verified using a similar procedure by measuring if the inter-planar spacings follow  
 175  $d_{\bar{1}100} \leq d_{\bar{1}010} = d_{01\bar{1}0}$ .

176 This then allows the least square method as mentioned above for  $a$ -plane system to be used  
 177 to estimate the lattice parameters for  $m$ -plane nitrides.

178 **4. Estimation of Al content**

For completely relaxed  $\text{Al}_x\text{Ga}_{1-x}\text{N}$  films the solid phase Al content ( $x_{solid}$ ) can be estimated by measuring either the  $a$  or  $c$  lattice parameter, subject to the validity of Vegard's law

$$a_0 = x.a_A + (1-x).a_G \quad (3a)$$

$$c_0 = x.c_A + (1-x).c_G \quad (3b)$$

<sup>179</sup> Here  $(a_G, c_G)$  and  $(a_A, c_A)$  are the lattice parameters of relaxed GaN and AlN respectively.  
<sup>180</sup> Rewriting the above equations

$$x = (a_G - a_0)/(a_G - a_A)$$

$$x = (c_G - c_0)/(c_G - c_A)$$

<sup>181</sup> Ideally, the  $x$  value calculated by using either the  $a$ - or  $c$ -lattice parameters should be the same. But in practice for epitaxial AlGaN these values differ. As we have seen in Sec.3 the AlGaN epilayers have thermal and lattice mismatches with the buffer/substrate which cause deformation/distortion in the wurtzite unit cell. For accurate estimation of  $x_{solid}$  using lattice parameters it is hence necessary to take into account the in-plane strain effect caused by buffer/substrate.

#### <sup>187</sup> 4.1. stress-strain tensor matrix

<sup>188</sup> Considering the  $X$ -axis along  $[1\bar{1}20]$ ,  $Y$ -axis along  $[1\bar{1}00]$  and  $Z$ -axis along  $[0001]$  direction,  
<sup>189</sup> the strain-stress relation for hexagonal crystals with a  $C_{v6}$  symmetry can be expressed as [14]

$$\begin{pmatrix} \sigma_{xx} \\ \sigma_{yy} \\ \sigma_{zz} \\ \sigma_{xz} \\ \sigma_{yz} \\ \sigma_{xy} \end{pmatrix} = \begin{pmatrix} C_{11} & C_{12} & C_{13} & 0 & 0 & 0 \\ C_{12} & C_{11} & C_{13} & 0 & 0 & 0 \\ C_{13} & C_{13} & C_{33} & 0 & 0 & 0 \\ 0 & 0 & 0 & C_{44} & 0 & 0 \\ 0 & 0 & 0 & 0 & C_{44} & 0 \\ 0 & 0 & 0 & 0 & 0 & C_{66} \end{pmatrix} \begin{pmatrix} \epsilon_{xx} \\ \epsilon_{yy} \\ \epsilon_{zz} \\ \epsilon_{xz} \\ \epsilon_{yz} \\ \epsilon_{xy} \end{pmatrix}$$

<sup>191</sup> where  $C_{ij}$  are the stiffness constants.

<sup>192</sup> For  $c$ -plane nitrides system the crystal is free along  $[0001]$ -direction (or Z-axis), so  $\sigma_{zz} = 0$   
<sup>193</sup> and

$$\epsilon_{zz} = -\frac{C_{13}}{C_{33}}(\epsilon_{xx} + \epsilon_{yy}) \quad (4a)$$

<sup>194</sup> For  $a$ -plane nitride epilayers the crystal is free along  $[1\bar{1}\bar{2}0]$ -direction (or  $X$ -axis), so  $\sigma_{xx} = 0$   
<sup>195</sup> and

$$\epsilon_{zz} = -\frac{C_{11}}{C_{13}}\epsilon_{xx} - \frac{C_{12}}{C_{13}}\epsilon_{yy} \quad (4b)$$

<sup>196</sup> For  $m$ -plane nitride epilayers the crystal is free along  $[\bar{1}100]$ -direction (or  $Y$ -axis), so  $\sigma_{yy} = 0$   
<sup>197</sup> and

$$\epsilon_{zz} = -\frac{C_{12}}{C_{13}}\epsilon_{xx} - \frac{C_{11}}{C_{13}}\epsilon_{yy} \quad (4c)$$

#### <sup>198</sup> 4.2. $c$ -plane AlGaN: effect of deformation on determination of Al content

We briefly review the well known case of  $c$ -plane oriented epilayers [5], where the in-plane strain is isotropic which deforms the unit cell, but maintains the hexagonal symmetry. So the strain values are

$$\epsilon_{xx} = \epsilon_{yy} = (a - a_0)/a_0, \quad \epsilon_{zz} = (c - c_0)/c_0$$

199 Substituting in eq(4a), we obtain

$$\frac{(a - a_0)}{a_0} + \gamma \frac{(c - c_0)}{c_0} = 0$$

200 Where  $\gamma = 2C_{13}/C_{33}$ . Substituting the expression for  $a_0$  and  $c_0$  and for small strain values,  
201  $x_{solid}$  can be expressed in terms of lattice parameters as

$$x = \frac{a(c_G - c) + \gamma(a_G - a)}{a(a_G - c_A) + \gamma(c_G - c_A)} \quad (5)$$

202 4.3. *a-plane AlGaN: effect of deformation on determination of Al content*

203 As discussed in Sec.3 *a*-plane nitride epilayers have in-plane anisotropic strain which distorts  
204 the basal plane. Hence, it is necessary to incorporate the effect of anisotropic strain to obtain a  
205 correct expression for Al content.

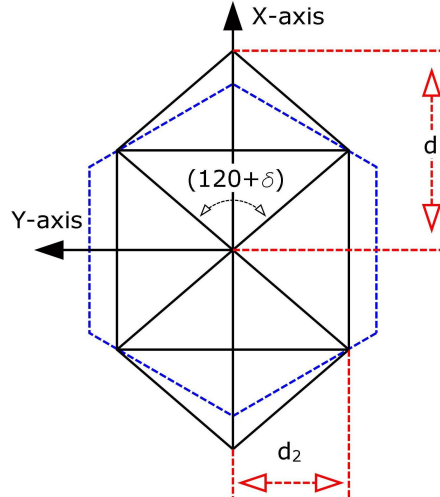


Figure 4: The dotted curve showing the basal plane of perfect hexagon and the solid curve same for distorted unit cell. Here  $1/2 d_1$  and  $d_2$  are the interplanar distance of  $(11\bar{2}0)$  and  $(\bar{1}100)$  planes respectively. These values can be estimated for the expression of  $d_{hkl}$  in eq.1

206 Here the strain values are

$$\begin{aligned}\epsilon_{xx} &= (d_1 - d_{10})/d_{10} \\ \epsilon_{yy} &= (d_2 - d_{20})/d_{20} \\ \epsilon_{zz} &= (c - c_0)/c_0\end{aligned}$$

207 where  $d_1 = 2d_{11\bar{2}0} = (2a \sin \gamma) / \sqrt{2(1 - \cos \gamma)}$  and  $d_2 = d_{1\bar{1}00} = (a \sin \gamma) / \sqrt{2(1 + \cos \gamma)}$  are as indicated in the schematic diagram of the distorted basal plane in Fig. 4. The additional subscript  
208 ‘0’ stands for relaxed AlGaN. Substituting these values into eqn. (4b) we obtain:  
209

$$\frac{c - c_0}{c_0} + \gamma_1 \frac{d_1 - d_{10}}{d_{10}} + \gamma_2 \frac{d_2 - d_{20}}{d_{20}} = 0$$

210 Assuming small strain and small distortion ( $|\delta| \leq 1^0$ ), this we obtain

$$x = \frac{(c_G - c)d_1d_2 + \gamma_1(d_{1G} - d_1)cd_2 + \gamma_2(d_{2G} - d_2)cd_1}{(c_G - c_A)d_1d_2 + \gamma_1(d_{1G} - d_{1A})cd_2 + \gamma_2(d_{2G} - d_{2A})cd_1} \quad (6)$$

211 where the additional subscripts ‘G’ and ‘A’ stand for GaN and AlN respectively, and  $\gamma_1 = C_{11}/C_{13}$   
 212 and  $\gamma_2 = C_{12}/C_{13}$ . For *m*-plane AlGaN the expression of *x* has a similar form except with  
 213  $\gamma_1 = C_{12}/C_{13}$  and  $\gamma_2 = C_{11}/C_{13}$ .

214 *4.4. Example - solid phase Al composition for a-plane AlGaN*

215 Following the procedure described in the previous section, we have estimated the lattice  
 216 parameters and solid phase Al composition for the series of *a*-plane AlGaN samples grown over  
 217 the entire composition range. The details of the lattice parameters derived from HRXRD and  
 218 the corresponding  $x_{solid}$  calculated are shown in Table 4. This also shows the values of  $x_{solid}$   
 219 derived independently from optical transmission measurements

Table 4: Comparison between *x*-values obtained from X-ray and transmission.

$x_{gas}$	<i>a</i> (Å)	<i>c</i> (Å)	$\gamma$ (degree)	<i>d</i> <sub>1</sub> (Å)	<i>d</i> <sub>2</sub> (Å)	$x_{solid}$ (XRD)	$x_{solid}$ (Trans.)
0.0	3.1960	5.1785	119.64	3.2132	2.7628	0.00	0.00
0.2	3.1783	5.1507	119.67	3.1940	2.7479	0.18	0.19
0.4	3.1608	5.1050	119.68	3.1762	2.7328	0.38	0.39
0.5	3.1535	5.0928	119.70	3.1654	2.7269	0.46	0.48
0.7	3.1362	5.0532	119.78	3.1466	2.7130	0.66	0.66
1.0	3.1116	4.9777	120.02	3.1107	2.6950	1.00	1.00

220 The measurement shows that the value of  $x_{solid}$  estimated from XRD and optical transmission  
 221 agrees within  $\pm 2\%$ . The  $x_{solid}$  is slightly lower than the  $x_{gas}$  because of parasitic reaction between  
 222 TMAI and NH<sub>3</sub>. A detailed discussion of the variation of strain and distortion with Al-content,  
 223 and its effect on the microstructure is discussed in references [10] and [11], and is not presented  
 224 here as the emphasis of this work is to discuss the procedure rather than the results.

225 **5. Conclusion**

226 In conclusion, we have observed that the anisotropic in-plane strain results in an orthorhom-  
 227 bic distortion in the wurtzite unit cell for non-polar *a*-plane nitrides. We have suggested a quick  
 228 method for confirming such a distortion to be orthorhombic, and derived an expression for *d*<sub>hkl</sub>  
 229 value for such distorted unit cells. We have also provided relatively simple procedure for esti-  
 230 mation of accurate lattice parameters using multiple reflections and minimizing the error by a

231 least square method. Since the orthorhombic distortion creates a difficulty for estimating group  
232 III content in ternary alloys, we have presented a technique which estimates the the correct Al  
233 content in *a*-plane AlGaN films taking into account the effect of anisotropic strain. We have  
234 also shown that this method is equally applicable for *m*-plane nitrides as well. These procedure  
235 should be valuable to researchers working on a wide range of non-polar III-nitride epilayers.

236 **References:**

237 **References**

- 238 [1] J. S. Im, H. Kollmer, J. Off, A. Sohmer, F. Scholz, and A. Hangleiter Phys. Rev. B  
239 **57**,(1998) R9435.
- 240 [2] R. Cingolani, A. Botchkarev, H. Tang, H. Morkoc, G. Traetta, G. Coli, M. Lomascolo, A.  
241 Di Carlo, F. Della Sala, and P. Lugli, Phys. Rev. B **61**, (2000) 2711.
- 242 [3] T. Paskova Phys. Stat Sol. (b) **245**, (2010) 1011.
- 243 [4] V. Darakchieva, P. P. Paskov, T. Paskova, E. Valcheva, and B. Monemar M. Heuken, Appl.  
244 Phys. Lett. **82**, (2003) 703.
- 245 [5] H. Angerer, D. Brunner, F. Freudenberg, O. Ambacher, M. Stutzmann R. Hopler, T. Metzger,  
246 E. Born, G. Dollinger, A. Bergmaier, S. Karsch, and H. J. Korner, App. Phys. Lett  
247 **71**, (1997) 1504.
- 248 [6] M. A. Moram, M. E. Vickers Rep. Prog. Phys. **72**, (2009) 036502.
- 249 [7] M.A. Moram, C.F. Johnston, J.L. Hollander M.J. Kappers, and C.J. Humphreys, J. Appl.  
250 Phys. **105**, (2009) 113501.
- 251 [8] V. Darakchieva, T. Paskova, M. Schubert, H. Arwin, P.P. Paskov, B. Monemar, D. Hommel,  
252 M. Heuken, J. Off, F. Scholz, B.A. Haskell, P.T. Fini, J.S. Speck and S. Nakamura, Phys.  
253 Rev. B **75**, (2007) 195217.
- 254 [9] C. Roder, S. Einfeldt, S. Figge T. Paskova, D. Hommel, P.P. Paskov, B. Monemar, U. Behn,  
255 B.A. Haskell, P.T. Fini, and S. Nakamura, J. Appl. Phys. **100**, (2006) 103511.
- 256 [10] M. R. Laskar, T. Ganguli, A. A. Rahman, A. P. Shah, M. R. Gokhale, A. Bhattacharya,  
257 Phys. Stat Sol. (RRL) **4**, (2010) 163.
- 258 [11] M. R. Laskar, T. Ganguli, N. Hatui, A. A. Rahman, M. R. Gokhale, A. Bhattacharya,  
259 Submitted to J. Cryst. Growth (2010).
- 260 [12] Elements of X-ray Diffraction. B. D. Cullity. Addison-Wesley. page 30 and Appendix 1.

- <sub>261</sub> [13] P. F. Fewster, N. L. Andrew J. Appl. Cryst. **28** (1995) 451.
- <sub>262</sub> [14] Group III Nitride Semiconductor Compound - Physics and Applications. Bernard Gil.  
<sub>263</sub> Clarendon Press - Oxford. page 316.